Ibn Al-Haitham Journal for Pure and Applied Sciences
Journal homepage: jih.uobaghdad.edu.iq
PISSN: 1609-4042, EISSN: 2521-3407
IHJPAS. 2024, 37(3)

Electropolymerization of Limonene and Its Nanocomposites with ZnO and TiO_2 to Protect Stainless Steel 304L Alloy from Corrosion in 3.5% NaCl Solution

Ayat Monther alqudsi[1*] and khulood Abid Saleh[2]
[1,2] Department of Chemistrry, College of Sciences, University of Baghdad, Baghdad, Iraq.
*Corresponding Author.

Received: 3 February 2023 Accepted: 8 May 2023 Published: 20 July 2024
doi.org/10.30526/37.3.3267

Abstract

The surface disintegration of metals and alloys in a particular surrounding environment is known as corrosion, in addition to its chemical qualities, corrosion processes change the physical and mechanical properties of a metal alloy. A new approach based on a unique material has been employed to prevent rusting. Conducting polymer-composites are material types that show promise for anticorrosion by electrochemical synthesis of polylimonene/metals oxide nanocomposite (ZnO,TiO_2) on Stainless Steel 304L, which plays as the working electrode by using the electropolymerization technique. The synthesized coating polymer was characterized by Fourier transform-infrared spectroscopy and atomic force microscopy checkups. The findings demonstrated that, when compared to the blank SS304L, PL/nanocomposite and PL provide the strongest corrosion defenses for the metal. The results explained that the corrosion protection increased from 52% for PL film to 89% for PL/ZnO film and to 97% for PL/TiO_2 at 298K. In addition, calculations were made for the kinetic and thermodynamic parameters (Ea, A, ΔH, and ΔS). Escherichia coli and Staphylococcus aureus, two gram-positive and gram-negative bacteria, were used to test the biological activity of polymeric film (E.Coli).

Keywords: Limonene, electropolymerization, corrosion, nanocomposite, polyeugenol.

1. Introduction

In the electrochemical polymerization process, the monomer is first oxidized to generate radicals, which are then combined with other radical cations or with another monomer to form radical dimers and longer chain lengths [1,2]. On the working electrode (WE), which is constructed of diverse materials such as stainless steel and glass with an indium tin oxide coating, monomer oxidation took place. To minimize costly and harmful damage, corrosion mitigation techniques that prevent and control corrosion have been developed. These techniques aim to eliminate or reduce the impact that corrosion has on public safety, the economy, and the environment [3].

The introduction of a novel conductive covering with particular properties may create new opportunities for optimizing a potential strategy [4].

Conductive polymers are widely employed in a variety of applications, including biochemical analysis, the fabrication of indicators and ion-selective electrodes, rechargeable batteries, chemical transistors, biorechargeable batteries [5], electrochromic devices [6], electro-luminescence [7], and dye-sensitive solar cells (DSSCs) [8].

Materials based on nano oxide-polymer composites are widely used in corrosion-protective coating applications [9,10]. The d-limonene (1-methyl-4-(1-methylethenyl) cyclohexane) is a monocyclic monoterpene that is a critical component of many citrus oils and has a lemony smell (orange, lemon, mandarin, lime, and grapefruit) [11]. Due to its pleasant citrus scent, d-limonene is commonly used as a flavor and aroma component in perfumes, cosmetics, foods, chewing gum, and beverages. Gallstones containing cholesterol have been medically treated by dissolving them with d-limonene, a suitable cholesterol solvent. Because it maintains healthy peristalsis and neutralizes stomach acid, it has also been used to treat heartburn. It has been demonstrated that d-limonene has chemopreventive effects against a number of cancers, including breast cancer and colorectal cancer [12]. According to Haider A. and Kholoud A., eugenol polymerized on titanium alloys before and after micro-arc oxidation was proven to be corrosion-resistant, and the protection efficiency (I%) improved to 81% at 323K. The samples' antibacterial activity was tested against a variety of oral fungi and bacteria. Polyeugenol (PE) coating has antibacterial efficacy against S. aureus and B. subtilis, as well as antifungal activity against the oral fungi Candida albicans and Candida glabrata [13]. Many researchers have polymerized limonene in different chemical ways, including Edison Rogerio and Ronierik Pioli, who first investigated and polymerized limonene at low temperatures by photochemical radical polymerization utilizing a combination of type II photoinitiators and alkyl halide initiators [14]. Tim Stober at el. Synthesizes two polymers, poly(cyclohexadiene carbonate) (PCHDC) and poly(limonene carbonate) (PLC), from carbon dioxide, cyclohexadiene oxide, and limonene oxide by a photoinitiated reaction with an initiator. The obtained materials have been examined for coating applications, exhibit promising solvent resistance and hardness, and may be utilized to manufacture scratch-resistant coatings in the future [15]. Saleem R. et al. studied the polymerization of biomass-based monomers, which leads to a multitude of new materials that can be applied in drug delivery, biology, nano-composites, adsorption and absorption, wastewater treatment, and other applications on small length scales [16]. In this work, stainless steel 304L (SS304L) alloys are electropolymerized by forming a thin layer of polylimonene (PL) on their surface using an alkaline electrolyte. The electrosynthesis of PL coatings was examined using FT-IR spectroscopy for Limonene and PL and by AFM measurements used to characterize PL and its composites with ZnO and TiO_2, and the coating adhesive was assessed to ascertain their surface morphologies. Investigations were also done on the biological effectiveness of PL covering against bacteria.

2. Materials and Methods

2.1 Materials

The chemical used in this study, molecular formula, suppliers, and purity are illustrated in **Table 1**.

Table 1. The Chemical materials were used

Raw Material	Molecular Formula	Supplier	Purity
Limonene	$C_{10}H_{16}$	Sigma-Aldrich	98%
Zinc oxide	ZnO	Hongwe nanometer	99%
Titanium oxide	TiO_2	Hongwe nanometer	99%
Oxalic acid	$H_2C_2O_4$	BDH	99%
Sodium chloride	NaCl	BDH	99.5%
Sodium hydroxide	NaOH	BDH	99%
Sulpharic acid	H_2SO_4	GCC	98%

2.2 Electrochemical polymerization process

The electropolymerization process of limonene is demonstrated in **Figure 1 and Eq 1**. On the S.S. 304L working electrode (anode) (containing 0.019 wt% (C), >0.50 wt% (Si), 1.53 wt% (Mn), 18.20 wt% (Cr),>0.030 wt wt% (P), 8.04 wt% (Ni), 0.030 wt% (S), and iron (Fe), the remainder was graded with carbide silicon (2000 mesh) and cleaned with D.W. and acetone. The SS304L placed in 0.1M NaOH containing 10 mM Limonene with three drops of H_2SO_4 (99%) and 0.1 g of oxalic acid as a supporting electrolyte and used a large rod of graphene as the counter electrode (cathode). The voltage of (0.85 mV) was applied at room temperature for a duration of 90 minutes; then, the electrode was washed with distilled water and dried in a hot air dryer.

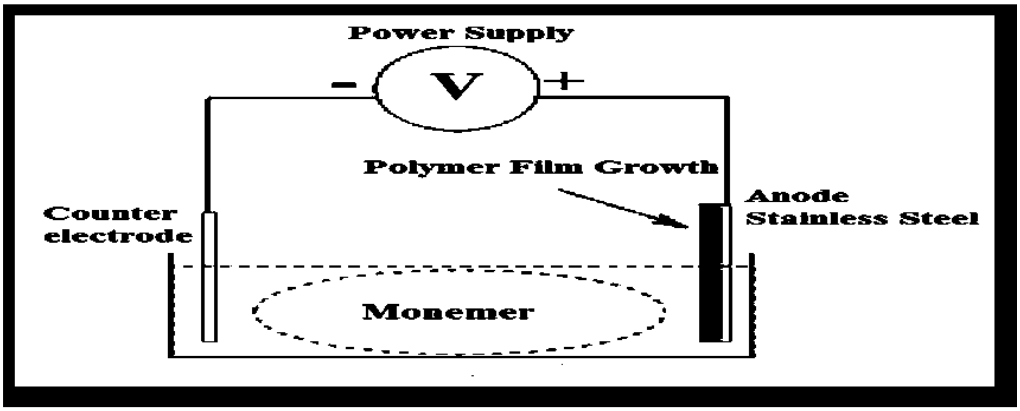

Figure 1. Electropolymerization process.

The potential of electropolymerization determined by cyclic voltammetry, as shown in **Figure 2**, is within the potential range of (-1000 to 1000) mV vs. the standard calomel electrode (SCE). All measurements were made in a solution containing 3.5% NaCl and were done between 298 and 328 K. Then 0.01g of ZnO and TiO_2 were also added to the monomer, repeating the electrochemical polymerization in the presence of these nano-oxides.

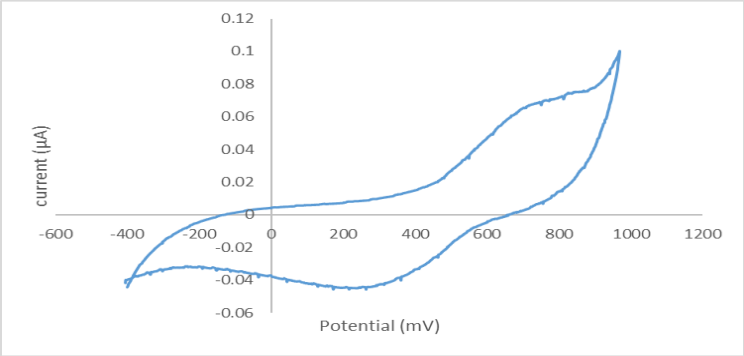

Figure 2. The cyclic voltammogram of PL.

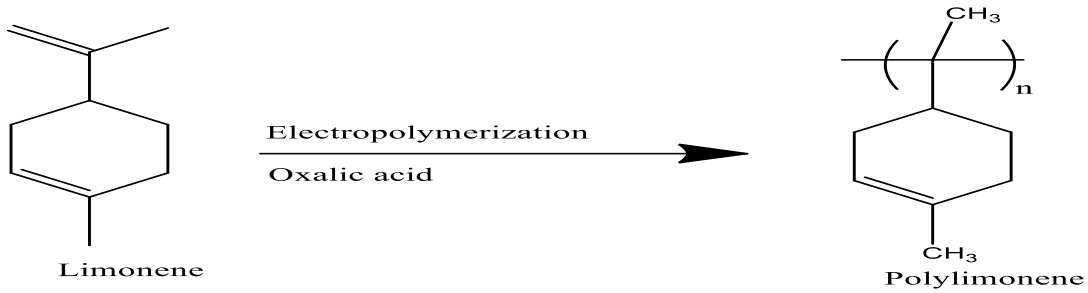

Eq 1. Electropolymerization of the Limonene to polymer**.**

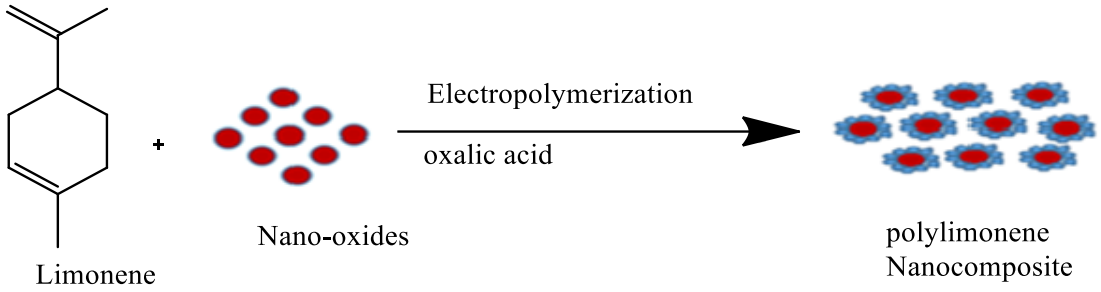

Eq 2. Electropolymerization of the Limonene with nano-oxides to polymer composite.

2.3 Corrosion Study

Three electrodes have been used in a corrosion study: a working electrode (SS 304L coated or uncoated), a reference electrode (SCE), and a counter or auxiliary electrode (platinum electrode). Under potentiostatic circumstances, coated and uncoated SS304L were subjected to anodic and cathodic polarization for the corrosion of SS304L at temperatures between (298 and 328) K.

2.4. Biological activity

In this study, the produced polymer (800 g/mL) was assessed for its biological activities toward both gram-positive and gram-negative bacteria, including *S. aureus* and *E. coli*. The synthesized PL's ability to inhibit bacteria was tested using the good diffusion method, and the solvent of choice was dimethyl sulfoxide (DMSO) to prepare the PL solution.

3. Results

3.1. FT-IR Spectroscopy of the *(PL)*

The PL and Limonene monomers produced on an SS 304L alloy by electrochemical polymerization were studied using FT-IR spectra, which are shown in **Figure 3**. The asymmetric C=C in Limonene is attributed to the absorption bands at 1669–1680 1680 cm^{-1} in **Figure 3**, although the IR spectra do not show this peak. The peak at around 3299 cm^{-1}, which is not present in the IR spectra of Limonene, may be ascribed to intramolecular H-bonds between the repeating units of PL chains.

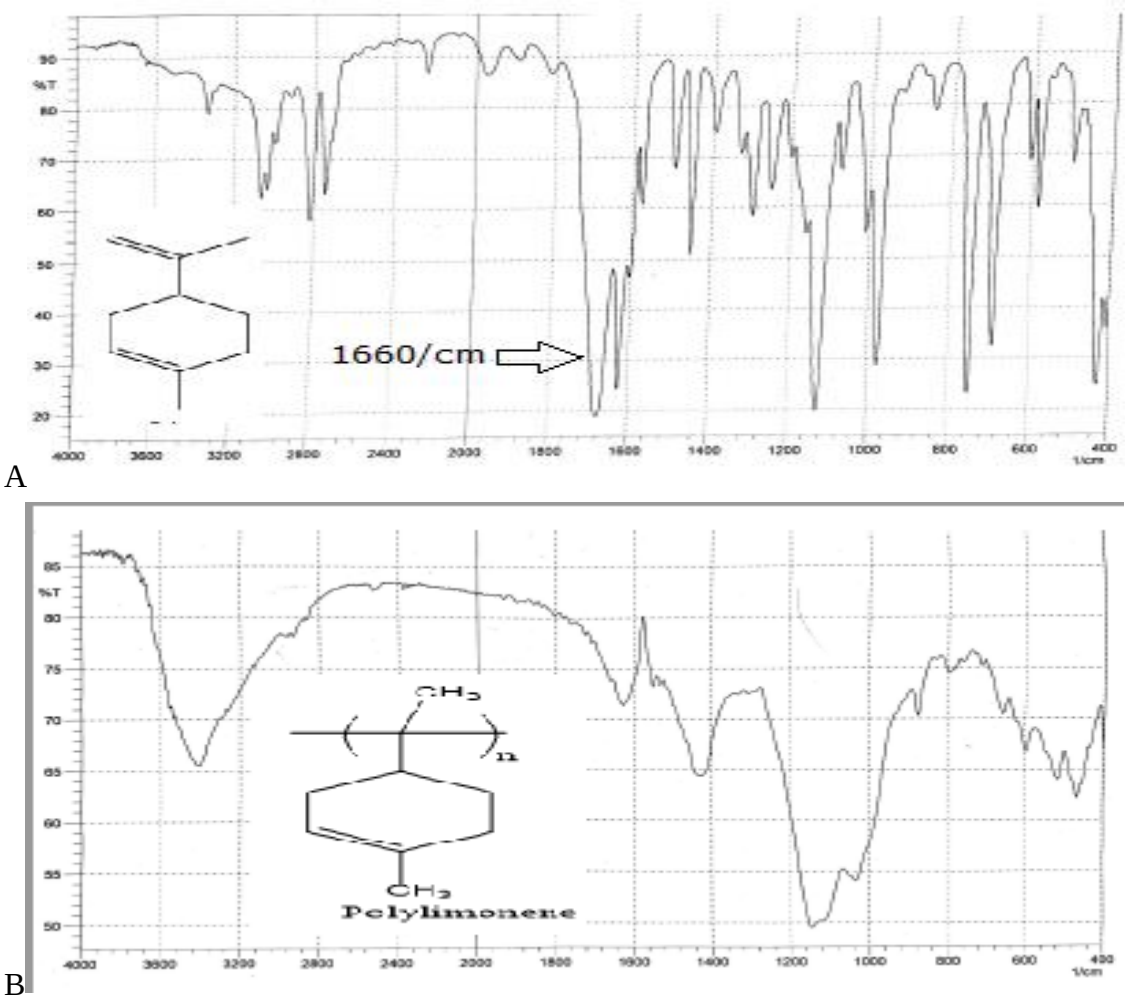

A

B

Figure 3. FT-IR images for A) Limonene, B) polylimonene**.**

3.2. AFM tests of PL and PL/ ZnO, TiO_2 composite:

The surface topography of SS304L coated with PL was examined using the AFM Technique. The most popular metrics for assessing the roughness of a surface using AFM analysis are the mean grain size (RMS) and roughness average (Ra). According to the findings, as shown in **Table 3**, the use of nanoparticles (NPs) reduced the grain size of PL, resulting in a reduction in surface roughness for all coated films. Therefore, the less rough the surface, the greater the barrier effect for avoiding coating corrosion [17,18].

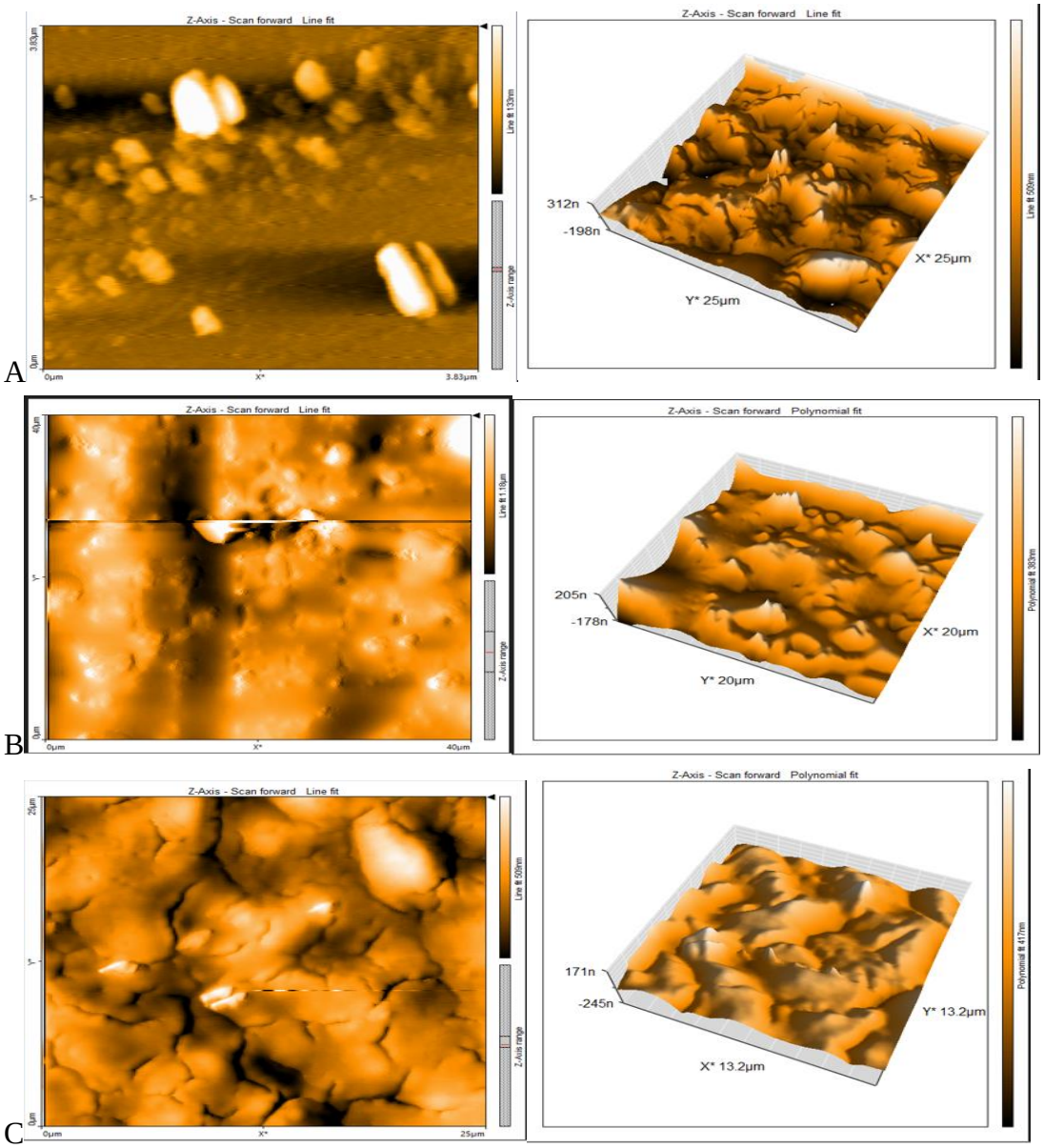

Figure 4. The AFM images for A) Polylimonene, B) PL+nano-ZnO , C) PL+nano-TiO_2.

Table 3. The AFM parameters to coated SS 304L with PL.

System	Ra (nm)	RMS (nm)	mean grain size (nm)
coated of PL	75.09	71.84	573
coated of PL modified by ZnO	61.02	51.34	519
coated of PL modified by TiO_2	49.05	40.65	589

4. Discussion

4.1. Corrosion measurements

Figure 5 depicts the effects of a polymeric layer in the absence and presence of nanomaterials on the cathodic and anodic curves of polarization of SS304L in a 3.5% NaCl solution at temperatures ranging from 298K to 328K. The corrosion current density was computed using extrapolated Tafel lines. **Table 3** shows the corrosion characteristics, which include the corrosion potential (E_{cor}), cathodic Tafel slope (β_c), corrosion current density (I_{cor}), and anodic Tafel slope (β_a). The protection efficiency is calculated using the following equation

[17]:

Protection efficiency

$$(PE\%)=[(I_{cor.})_{uncoated}-(I_{cor.})_{coated}]/(I_{cor.})_{uncoated} \quad (3)$$

Where the corrosion current density for coated SS304L is represented by $(I_{cor.})$ uncoated. After incorporating the nanomaterials, the corrosion potential (E_{cor}) was shifted to more positive values (i.e., in a noble direction), and I_{cor} decreased. The Stern-Gerry equation has been used to calculate the resistance of polarization (Rp) [18]:

$$Rp=(\beta_a+\beta_c)/[2.303(\beta_a\beta_c)]*I_{COR.} \quad (4)$$

The conditions for measuring polarization resistance (Rp) are comparable to those for complete polarization curve measurements, and it has been deemed useful as one way to spot corrosion upsets and start fixing them [19]. The values of Rp are shown in **Table 3**.

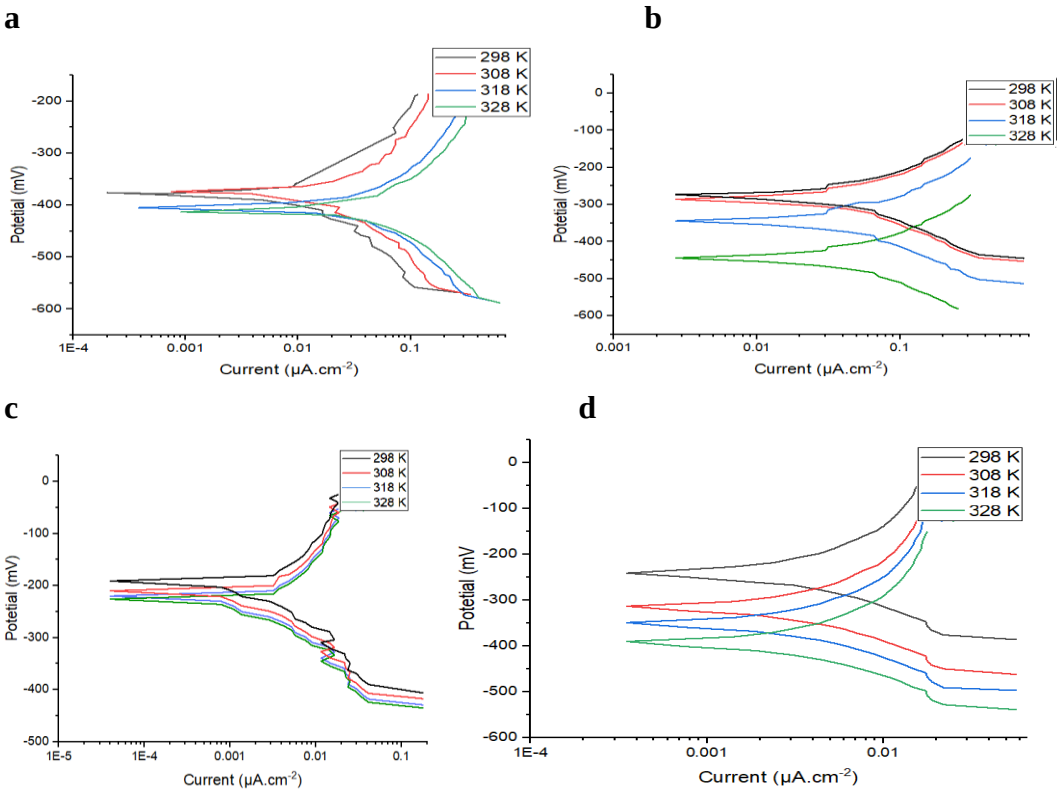

Figure 5. Tafel curves for corrosion of a. uncoated SS304L, b. coated SS304L with PL, c.coated SS304L with PL/ZnO , d. coated SS304L with PL/TiO_2.

The findings in **Table 3** show the protection efficiency (PE%), which has been demonstrated to be significantly influenced by temperature, with PE% values rising as temperature increases. This might be explained by the fact that the boundary layer's thickness increased with temperature [19].

Table 3 shows that the WL and PL values were highly dependent on temperature. Temperature influenced the WL and PL values, which increased as the temperature rose. All coating systems exhibited the highest WL and PL values at 328K. WL and PL values were also lower in coated SS 304L than in uncoated SS304L, and these values were obviously lower after adding nanomaterial. The porosity of the coated layer and the coating's ability to hinder [20,26].

Table 3. Corrosion values for uncoated and coated SS304L alloy by PL.

T(K)		*E_{cor} (mV)*	*i_{corr} ($\mu A/cm^2$)*	*-βc (mV/ Dec)*	*βa (mV/ Dec)*	*WL(g/m2.d)*	*Rp (Ω/cm2)*	*PL (mm/y)*	*PE %*
Uncoated	298	376	8.78	124.2	130.5	2.2	3147.13	$9.79*10^{-2}$	-
	308	374	21.47	160.8	155.0	5.38	1596.17	$2.40*10^{-1}$	-
	318	394	36.95	177.2	170.4	10.3	1020.81	$4.57*10^{-1}$	-
	328	405	49.57	192.1	190.4	15.4	837.62	$6.87*10^{-1}$	-
Coated PL	298	280	4.16	36.1	40.4	1.29	1989.93	$5.76*10^{-2}$	52
	308	291	6.48	61.2	45.4	1.62	1746.55	$7.23*10^{-2}$	69
	318	283	10.37	52.7	41.1	2.6	966.88	$1.16*10^{-1}$	71
	328	271	17.14	76.2	71.6	4.3	935.16	$1.91*10^{-1}$	72
Coated PL+ ZnO EECS	298	237	$917.46*10^{-3}$	63.8	72.8	$2.3*10^{-1}$	1610.04	$1.02*10^{-2}$	89
	308	237	1.31	79.7	89.8	$3.28*10^{-1}$	1399.58	$1.46*10^{-2}$	93
	318	211	1.87	90.7	101.7	$4.68*10^{-1}$	1113.23	$2.08*10^{-2}$	95
	328	202	2.92	93.8	116.9	$7.31*10^{-1}$	773.88	$3.25*10^{-2}$	94
Coated PL+TiO2	298	242	$623.09*10^{-3}$	43.9	56.7	$1.56*10^{-1}$	17242.68	$6.95*10^{-3}$	97
	308	301	$950.47*10^{-3}$	49.8	49.6	$2.38*10^{-1}$	11352.52	$1.06*10^{-2}$	96
	318	324	1.43	59.6	59.2	$3.59*10^{-1}$	9018.235	$1.60*10^{-2}$	91
	328	342	2.67	72.1	64.5	$6.7*10^{-1}$	5536.548	$2.98*10^{-2}$	90

4.2. Thermodynamics and kinetics studies of coated SS304L

Using a comparable Arrhenius equation, the influence of temperature on the corrosion rate of uncoated and coated SS304L in a 3.5% NaCl solution was examined [21, 27]

$$Ic_{OR.}=Ae^{-Ea/RT} \quad (5)$$

Where Ic_{OR} and A are the current density of corrosion and Arrhenius factor respectively. Ea (J moL^{-1}) is the activation energy, T (K) is the temperature, and R shows the global constant (J $moL^{-1}K^{-1}$)

Equation 5 has been converted to logarithm form

$$\text{Log } Ic_{OR.}=\text{Log A}-(Ea / 2.303RT) \quad (6)$$

The activation energy was determined from the plot that represents the relationship between Log I_{COR}. and the reciprocal of the absolute temperature (1/T), as shown in Figure (5.a).

The transition state equation is shown below**:**[22]

$$\log (Ic_{OR.}/ T) = [\log (R / Nh)] + [\Delta S / 2.303 R]– [\Delta H / 2.303 RT] \quad (7)$$

Where h is the Planks constant (6.62 10^{-34} J.S.) and N is the Avagadro's number (6.022×10^{23} mol). The graphic showing the connection between log (I_{COR}/T) and the reciprocal of the absolute temperature (1/T) was used to calculate the entropy of activation ΔS* and enthalpy of activation ΔH*, as seen in **Figure 5.b** where the intercept is (Log) and the slope is (-ΔH*/2.303RT), (R/Nh) + ΔS*/2.303R).

The activation parameters of thermodynamic and kinetic corrosion (Ea, A, and H*) are typically lower SS304L coated with PL and PL/ZnO,TiO_2 compared to for uncoated SS304L, indicating a decrease in the number of corrosion active sites on the surface of 304L [22, 23]. All the samples have a negative activation entropy, which means that association rather than dissociation was used to determine the step's rate and that the disorder associated with the change from reactants to activated complex has decreased [24, 25].

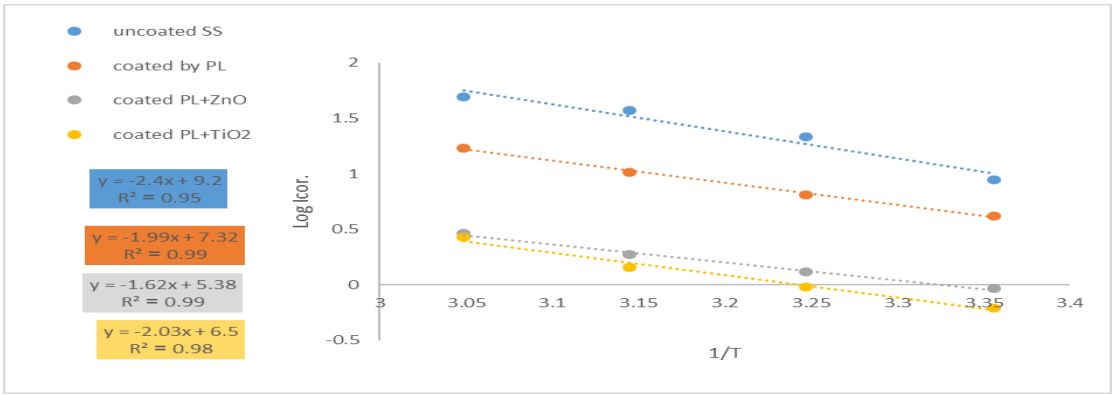

A

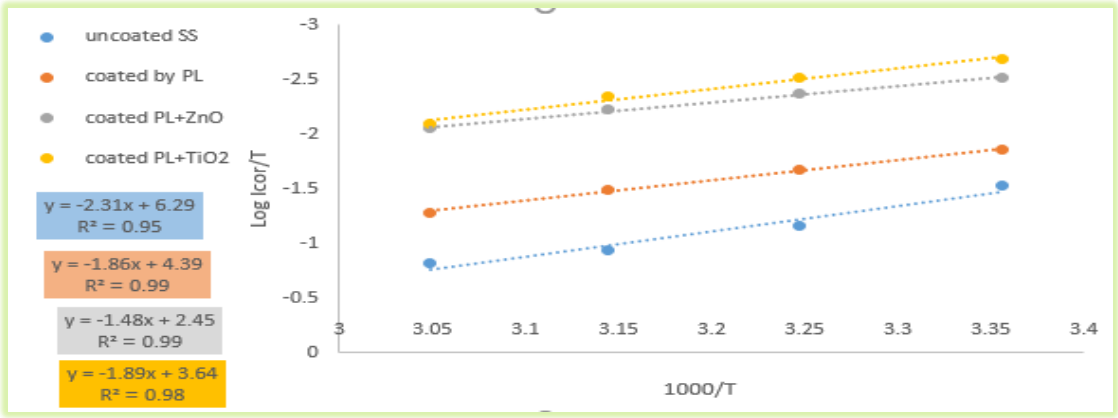

B

Figure 5. a-Plot of (log Icor.) vs. (1/T) for SS 304L with coating by PL/ZnO,TiO_2, b-Plot of (log $I_{COR.}$/T) vs (1/T) for SS304L with coating by PL/ZnO,TiO_2.

Table 4. The values of kinetic and thermodynamic for all cases.

	ΔH (KJ/mol)	**-ΔS (J/mol.K)**	**Ea (kJ/mol)**	**A (Molecule. cm^{-2} .S^{-1})**
Uncoated SS304L (blank)	44.24	77.17	45.92	9.5X10^{32}
Coated SS304L coated by PL	35.47	11356	53.62	1.26X10^{31}
Coated SS304L by PL/ZnO	28.14	150.71	31.20	2.4X10^{28}
Coated SS304L by PA/ TiO_2	34.5	127.29	38.87	1.9X10^{30}

4.3. Antibacterial study

The inhibitory zones of the polymers generated have been evaluated on both bacteria species (*S. aureus and E. coli*) for PL and PL/ZnO,TiO_2 at a concentration of 800g/ml. DMSO was utilized as the solvent. Table 6 summarizes the findings.

Table 5. The PL and PL/ZnO,TiO_2 inhibition zone

Coating SS 304L by:	***S. aureus* (+Gram)**	***E. coli* (-Gram)**
PL	20	20
PL modified by ZnO	24	30
PL modified by TiO_2	24	28
Amoxicillin	30	30
DMSO	-	-

The polymer has shown superior inhibitory effectiveness against both *S. aureus* and *E. coli* when compared to amoxicillin. The polymer's capacity to kill bacteria is determined by its ability to create a stable interaction complex with drug-bound topoisomerases and cleaved DNA. The polymer's suppression of topoisomerase activity and formation of stable complexes with DNA have a significant detrimental impact on cell oxides. Nanomaterials are becoming more important in medical, pharmaceutical, and biological uses as an antibacterial method in opposition to the spread of antibiotic-resistant bacteria and the resurgence of infectious illnesses. NPs are assumed to be biocidal effective due to their tiny size and high surface-to-volume ratio, which enable them to come into contact with the membranes of microorganisms [28-32].

5. Conclusion

At rising temperatures, both the corrosion potential (E_{cor}) and corrosion current density (I_{COR}) increased. In both the presence and absence of the nanomaterial, the corrosion current density (I_{COR}) decreased after covering the SS304L with the polymer film. Tafel plots showed that the corrosion potential (E_{cor}) of the SS304L coated with the polymer film changes to a higher position as compared to that of the uncoated SS304L in the absence and presence of the nanomaterial, indicating that the polymer film functions as an anodic protection. For the uncoated and coated SS304L in the absence and presence of the nanomaterial, PE% declined with rising temperature. ZnO-modified polymer film-coated SS304L showed greater PE% than TiO_2-modified polymer film-coated SS304L. The AFM investigation revealed that the creation of a protective coating on the metal surface was what caused SS304L to be protected. In addition to corrosion resistance, the polymer film has antimicrobial properties against the bacterium S. aureus and E. coli, with the polymer film enhanced with NPs having particularly potent antibacterial properties.

Acknowledgment

The authors thank the Department of Chemistry, College of Science, University of Baghdad for research approval.

Conflict of Interest

The authors declare that they have no conflicts of interest.

Funding

There is no funding for the article.

References

1. Zhan, C.; Yu, G.; Lu, Y.; Wang, L.; Wujcik, E.; Wei, S. Conductive Polymer Nanocomposites: A Critical Review of Modern Advanced Devices. *Journal of Materials Chemistry* **2017**, *5*(*7*), 1569-1585. https://doi.org/10.1039/C6TC04269D.
2. Contal, E.; Lakard, S.; Dumur, F.; Lakard, B. Investigation of Polycarbazoles Thin Films Prepared by Electrochemical Oxidation of 3-and 9-Substituted Carbazoles. *Progress in OrganicCoatings* **2022**, *162*,106563. https://doi.org/10.1016/j.porgcoat.2021.106563.
3. Habeeb, S. A.; Saleh, K. A. Electrochemical Polymerization and Biological Activity of 4-(Nicotinamido)-4-Oxo-2-Butenoic Acid as an Anticorrosion Coating on A 316L Stainless Steel Surface. Iraqi Journal of Science **2021**, *3(62)*, 729-741. https://doi.org/10.24996/ijs.2021.62.3.3.
4. Hossen, A.; Mahmud, R.; Islam, A. Minimization of Corrosion in Aquatic Environment–A Review. *Int J Hydro* **2023**, *7(1)*, 9-16. https://doi.org/10.15406/ijh.2023.07.00334.
5. Decher, G.; Hong, J. D.; Schmitt, J. Buildup of Ultrathin Multilayer Films by a Self-Assembly Process: III. Consecutively Alternating Adsorption of Anionic and Cationic Polyelectrolytes on Charged Surfaces. *Thin solid films* **1992**, *210*, 831-835. https://doi.org/10.1016/0040-6090(92)90417-A.
6. Holder, E.; Tessler, N.; Rogach, A.L. Hybrid Nanocomposite Materials with Organic And Inorganic Components for Opto-Electronic Devices. *Journal of Materials Chemistry* **2008**, *18(10)*, 1064-1078. https://doi.org/10.1039/B712176H.
7. Steitz, R.; Jaeger, W.; Klitzing, R.V. Influence of Charge Density and Ionic Strength on the Multilayer Formation of Strong Polyelectrolytes. *Langmuir* **2001**, *17(15*), 4471-4474. https://doi.org/10.1021/la010168d.
8. Guo, Y.; Geng, W.; Sun, J. Layer-by-Layer Deposition of Polyelectrolyte−Polyelectrolyte Complexes for Multilayer Film Fabrication. *Langmuir* **2009**, *25(2)*, 1004-1010. https://doi.org/10.1021/la803479a.
9. Elzbieciak, M.; Zapotoczny, S.; Nowak, P.; Krastev, R.; Nowakowska, M.; Warszynski, P. Influence of Ph on The Structure of Multilayer Films Composed of Strong and Weak Polyelectrolytes. *Langmuir* **2009**, *25(5)*, 3255-3259. https://doi.org/10.1021/la803988k
10. Ali, M. I.; Saleh, K. A. Corrosion Protection Studies of Stainless Steel Alloy In Hydrochloric Acid by using Electropolymerized Poly (N-Imidazolyl Tetrahydrophthalamic Acid). *International Journal of Engineering & Technology* **2018**, *7(4)*, 5821-5828. https://doi,org/10.24996/ijs.2020.61.10.3
11. Wijayanti, W.; Sasongko, M.N. The Role of Limonene in The Branching of Straight Chains in Low-Octane Hydrocarbons. *Renewable Energy* **2023**, *204*, 421-431. https://doi.org/10.1016/j.renene.2023.01.008
12. Masood, A.; Ahmed, N.; Razip Wee, M.M.; Patra, A.; Mahmoudi, E.; Siow, K.S. Atmospheric Pressure Plasma Polymerisation of D-Limonene and its Antimicrobial Activity. *Polymers* **2023**, *15*(*2*), 307. https://doi.org/10.3390/polym15020307.
13. Al-Mashhadani, H.A.; Saleh, K.A. Electro-Polymerization of Poly Eugenol on Ti and Ti Alloy Dental Implant Treatment by Micro arc Oxidation using as Anti-Corrosion and Anti-Microbial. *Research Journal of Pharmacy and Technology* **2020**, *13*(*10*), 4687-4696. https://doi.org/10.5958/0974-360X.2020.00825.2.
14. De Oliveira, E.R.M.; Vieira, R.P. Synthesis and Characterization of Poly (Limonene) by Photoinduced Controlled Radical Polymerization. *Journal of Polymers and the Environment* **2020**, *28*, 2931-2938. httpa://doi,org/10.1007/s10924-020-01823-7.

15. Stoßer, T.; Li, C.; Unruangsri, J.; Saini, P. K.; Sablong, R. J.; Meier, M. A.; Koning, C. Bio-Derived Polymers for Coating Applications: Comparing Poly (Limonene Carbonate) and Poly (Cyclohexadiene Carbonate). *Polymer Chemistry* **2017**, *8(39)*, 6099-6105. https://doi.org/10.1039/C7PY01223C.
16. Raza, S.; Zhang, J.; Ali, I.; Li, X.; Liu, C. Recent Trends in the Development of Biomass-Based Polymers From Renewable Resources and their Environmental Applications. *Journal of the Taiwan Institute of Chemical Engineers* **2020**, *115*, 293-303. https://doi.org/10.1016/j.jtice.2020.10.013.
17. Al-Mashhadani, H.A.; Saleh, K.A. Electro-Polymerization of Poly Eugenol on Ti and Ti Alloy Dental Implant Treatment by Micro Arc Oxidation using as Anti-Corrosion and Anti-Microbial. *Res. J. Pharm. Technol* **2020**, *13(10)*, 4687-4696. https://doi.org/10.5958/0974-360X.2020.00825.2.
18. Liu, Y.; Guo, X.; Liu, D.; Wang, Y.; Hao, L.; Jin, Y; Wu, Y. C. Inhibition Effect of Sparteine Isomers With Different Stereochemical Conformations on the Corrosion of Mild Steel In Hydrochloric Acid Solution. *Journal of Molecular Liquids* **2022**, *345*, 117833. https://doi.org/10.1016/j.molliq.2021.117833
19. Lorenzetti, M.; Pellicer, E.; Sort, J.; Baró, M. D.; Kovač, J.; Novak, S.; Kobe, S. Improvement to the Corrosion Resistance of Ti-Based Implants Using Hydrothermally Synthesized Nanostructured Anatase Coatings. *Materials* **2014**, *7(1)*, 180 194. https://doi.org/10.3390/ma7010180.
20. Li, Z.; Yuan, X.; Sun, M.; Li, Z.; Zhang, D.; Lei, Y; Wang, F. Rhamnolipid as an Eco-Friendly Corrosion Inhibitor for Microbiologically Influenced Corrosion. *Corrosion Science* **2022,** *204*, 110390. https://doi.org/10.1016/j.corsci.2022.110390.
21. Kassou, O.; Galai, M.; Ballakhmima, R. A.; Dkhireche, N.; Rochdi, A.; Ebn Touhami, M.; Zarrouk, A. Comparative Study of Low Carbon Steel Corrosion Inhibition in 200 Ppm Nacl by Amino Acid Compounds. *J. Mater. Environ. Sci* **2015**, *6(4)*, 1147-1155. https://www.researchgate.net/publication/274639114.
22. Kubba, R. M.; Mohammed, M. A.; Ahamed, L. S. DFT Calculations and Experimental Study to Inhibit Carbon Steel Corrosion in Saline Solution by Quinoline-2-One Derivative: Carbon Steel Corrosion. *Baghdad Science Journal* **2021**, *18(1)*, 0113-0113. http://dx.doi.org/10.21123/bsj.2020.18.1.0113.
23. Oliveira, M.; Moraes, J.; Faez, R. Impedance Studies of Poly (Methylmethacrylate-Co-Acrylic Acid) Doped Polyaniline Films on Aluminum Alloy. *Progress in Organic Coatings* **2009**, *65(3)*, 348-356. https://doi.org/10.1016/j.porgcoat.2009.02.003
24. Qin, W. Corrosion mechanisms of copper and gold ball bonds. In ISTFA ASM *International* **2022**, 318-322. https://doi.org/10.1149/1.3567681
25. Joseph, B.; John, S.; Joseph, A.; Narayana, B. Imidazolidine-2-Thione as Corrosion Inhibitor for Mild Steel in Hydrochloric Acid. **2010**, *17*, 274-366. https://nopr.niscpr.res.in/bitstream/123456789/10452/1/IJCT%2017(5)%20366-374.pdf.
26. Abdallah, M. Rhodanine Azosulpha Drugs as Corrosion Inhibitors for Corrosion of 304 Stainless Steel in Hydrochloric Acid Solution. *Corrosion science* **2022**, *44(4)*, 717-728. https://doi.org/10.1016/S0010-938X(01)00100-7.
27. Noor, E. ;Al-Moubaraki, A. H. Thermodynamic Study of Metal Corrosion and Inhibitor Adsorption Processes in Mild Steel/1-Methyl-4 [4′(-X)-Styryl Pyridinium Iodides/ Hydrochloric Acid Systems. *Materials Chemistry and Physics* **2008**, *110(1)*, 145-154. https://doi.org/10.1016/j.matchemphys.2008.01.028.
28. Li, Y.; Feng,T.; Wang, Y. The Role of Bacterial Signaling Networks in Antibiotics Response and Resistance Regulation.*Marine Life Science & Technology* **2022**, *4(2)*, 163-178. https://doi.org/10.1007/s42995-022-00126-1.
29. Abd El Rehim, S.S.; Hassan, H.H.; Amin, M.A. Corrosion inhibition of Aluminum by 1, 1 (lauryl amido) Propyl Ammonium Chloride in HCl Solution. *Materials chemistry and physics* **2001**, *70(1)*, 64-72. https://doi.org/10.1016/S0254-0584(00)00468-5

30. Saleh, K.A.; Ali, M.I. Electro Polymerization for (N-Terminal Tetrahydrophthalamic Acid) for Anti-Corrosion and Biological Activity Applications. *Iraqi Journal of Science* **2020**, 61(1), 1-12. https://doi.org/10.24996/ijs.2020.61.1.1
31. Mohammed, R.A.; Saleh, K.A. Conducting Poly [N-(4-Methoxy Phenyl) Maleamic Acid]/Metals Oxides Nanocomposites for Corrosion Protection and Bioactivity Applications. *Chem. Methodol* **2022**, *6(1)*, 74-82. https://doi.org/10.22034/chemm.2022.1.8
32. Mohammed, R.A.; Saleh, K.A. Electropolymerization of [N-(1, 3-thiazo-2-yl)] maleamic acid and their Nanocomposite with Graphene Oxide as Protective Coating against Corrosion and Antibacterial Action. *Iraqi Journal of Science* **2022**, *63(10)*, 4163-4174. https://doi.org/10.24996/ijs.2022.63.10.3